Marine Biology, in press
The original is available at www.springerlink.com
DOI 10.1007/s00227-007-0781-2

Growth and mortality rates of the fan mussel *Pinna nobilis* in Lake Vouliagmeni (Korinthiakos Gulf, Greece): a generalized additive modelling approach

Stelios Katsanevakis

Department of Zoology-Marine Biology, Faculty of Biology, University of Athens, Panepistimioupolis, 15784 Athens, Greece
e-mail: stelios@katsanevakis.com tel: +30-210-4203508 fax: +30-210-7274608

Abstract

The temporal patterns and the effect of shell size and depth on growth and mortality rates of the endangered fan mussel *P. nobilis* were investigated in the marine Lake Vouliagmeni (Korinthiakos Gulf, Greece). A total of 160 individuals were tagged and monitored monthly for a period of 17 months. At each visit, the size of the tagged individuals (shell width, *w*) was measured *in situ* and recorded. Any mortality event was also recorded and attributed to natural causes or (illegal) fishing. Growth and mortality rates were modelled with generalized additive models, which are non-parametric flexible models that free the researcher from the limiting concept of a strict parametric shape. The use of GAMs allowed the exploration of shapes of growth and mortality response curves in relation to predictor variables and allowed the fitting of statistical models that better agree with ecological theory. Growth rates had a seasonal pattern, with an extended period of very slow growth between late autumn and early spring, i.e. during the cold season, another short period of slow growth during August (when water temperatures reached their maximum values exceeding 29 ^{o}C), and a peak in growth rates during late spring – early summer, probably related to an optimum combination of temperature and food availability. Growth rates varied with shell size, with a peak at w ~ 4.5 cm, followed by a sharp decline to an approximately constant level, with sizes ranging from 9 to 15 cm, and a further decline with larger sizes down to almost zero for $w > 20$ cm. Growth rates did not vary substantially with depth. Although *P. nobilis* is a protected species in the EU and its fishing is strictly prohibited, fishing mortality was very high in Lake Vouliagmeni (much greater than natural mortality), especially during the hot season when the lake was crowded by summer visitors. The fan mussels were poached exclusively by free-diving and due to the high turbidity of the lake's water, fishing mortality was higher in shallow areas (and mostly for large individuals) and was practically zero at depths > 9 m. Due to fishing mortality, a size segregation of *P. nobilis* was observed in the lake: large individuals were restricted to deeper areas, while young and small individuals were more abundant in shallow areas where there was preferential recruitment. Natural mortality was strikingly size dependent and *P. nobilis* suffered high natural mortality during the first year of life; the probability of death by natural causes quickly diminished as the fan mussels grew in size. No depth-related differences in natural mortality were found.

Introduction

The fan mussel *Pinna nobilis* is endemic to the Mediterranean Sea. It is one of the largest bivalves of the world, attaining total anterio-posterior lengths of up to 120 cm (Zavodnik et al. 1991). It is long lived, living up to 20 years according to Butler et al. (1993), while in Thermaikos Gulf (Greece) an age of 27 years has been reported (Galinou-Mitsoudi et al. 2006). *P. nobilis* and some other pinnids such as *P. bicolor* display the fastest shell growth rates reported for any bivalve (Richardson et al. 2004). Its larval life spans 5 to 10 days (Butler et al. 1993), settlement occurs mostly during late summer and autumn (Richardson et al. 1999), and it has very variable recruitment. *P. nobilis* occurs in coastal soft-bottom areas at depths between 0.5 and 60 m, mostly in seagrass meadows but also in bare sandy bottoms (Katsanevakis 2006a). Fan mussels live partially buried by the anterior portion of the shell and

attached by their numerous byssus filaments to particles and solid structures of the substratum.

The global population of *P. nobilis* has been greatly reduced during the last few decades as a result of recreational and commercial fishing for food, use of its shell for decorative purposes, and incidental killing by trawling and anchoring. Consequently, it has been listed as an endangered species in the Mediterranean and is under strict protection according to the European Council Directive 92/43/EEC (Annex IV) and the national laws of most Mediterranean countries.

Our knowledge of the biology and ecology of the species is fragmentary and several aspects need further investigation (Butler et al. 1993; Ramos 1998; García-March et al. 2007a). Increasing information on its population biology and ecology is crucial to effectively protecting this endangered species. Studying the vital rates (growth, mortality and fecundity rates) of the species is necessary for modelling its population dynamics, which in turn is a prerequisite to proposing effective measures for the protection of the species.

There are only a few studies dealing with the absolute growth of the species in a number of Mediterranean sites that have either used size-at-age data (Richardson et al. 1999; Richardson et al. 2004; Galinou-Mitsoudi et al. 2006) or estimated growth by *in-situ* monitoring of tagged individuals (Moreteau and Vicente 1982; Šiletić and Peharda 2003; García-March et al. 2007a). The latter studies were based on increments of size over a period of usually one year or even as long as two years in the case of Šiletić and Peharda (2003). However, using such a long time span to measure the size increment may quite possibly produce a great bias in estimating the instantaneous growth rates, especially in young individuals (Yamaguchi 1975).

With either of the above approaches, only the mean annual growth was modeled, while the seasonal variation of growth was ignored and remained unmodeled. Seasonal variation of *P. nobilis* growth rates has only been estimated by Richardson et al. (1999), for two small fan mussels from Villaricos (Spain), for the first two years of life. They sampled U-shaped spines along the main axis of shell growth and conducted stable-isotope analyses of oxygen in shell carbonate to predict the in-situ temperature at the time of shell-carbonate deposition. Subsequently, calendar dates were assigned to the inferred temperature records; estimated dates of shell deposition at known shell sampling-positions allowed the calculation of skeletal growth rates.

All the abovementioned studies have assumed *a priori* that the von Bertalanffy growth model (VBGM) (Bertalanffy 1938) is the 'true' model describing *P. nobilis* growth. However, the practice of *a priori* using VBGM has often been criticized (e.g. Katsanevakis 2006b), and for many aquatic species, other models like Gompertz (Gompertz 1825) or the logistic model (Ricker 1975) better describe absolute growth. Specifically for bivalves, other models than VBGM often better fit the data and sigmoid growth curves seem to be quite common (Yamaguchi 1975). The underlying principle of the VBGM is that the growth rate tends to decrease linearly with size, as indicated in the differential equation $\frac{\mathrm{d}L}{\mathrm{d}t} = k_1(L_\infty - L)$, where L is the length (or generally a measure of the size of the species), k_1 (as well as k_2 and k_3 in subsequent equations) is a relative growth rate parameter (with units yr^{-1}) and L_∞ is the asymptotic length. The VBGM has no inflection point for $t > 0$ and its graph is concave downward. The Gompertz growth model (Gompertz 1825) is an alternative sigmoidal growth curve that assumes an exponential decrease of the growth rate with

size and is given by the differential equation $\frac{dL}{dt} = -k_2 L \ln\left(\frac{L}{L_\infty}\right)$. The logistic growth model (Ricker 1975) is also a sigmoid growth curve, in which the growth rate is given by the concave downward parabola $\frac{dL}{dt} = k_3 L\left(1 - \frac{L}{L_\infty}\right)$.

The above models give very different patterns of growth rate in relation to individual size. As an example, VBGM, Gompertz, and logistic models were fitted (Katsanevakis 2006b) to yellowfin tuna data (Lessa and Duarte-Neto 2004) and the resultant patterns are shown in Fig. 1; large model-dependent differences in estimated growth rates were found. Katsanevakis (2006b) proposed the use of many candidate growth models and a multi-model inference (MMI) approach, based on information theory (Burnham and Anderson 2002), as a more robust approach to study absolute growth and deal with model selection uncertainty. With MMI, the response variable is model-averaged based on 'Akaike' weights, which may be interpreted as a posterior probability distribution over the set of candidate models (Akaike 1983; Buckland et al. 1997; Burnham and Anderson 2002). Another approach would be not to adopt a specific parametric form, but to fit a flexible non-parametric model that could attain not only the forms of the abovementioned models but also any intermediate or even diverse form. All the frequently used growth models have strong and often simplistic underlying assumptions, while biological phenomena are usually quite complex and are being driven apart from the main dominant effects by many other smaller effects that are difficult to study. The variable environment, individual heterogeneity, and rare events that may have large effects add further complexity. In the present study, generalized additive models (GAMs; Hastie and Tibshirani 1990) were used, which is a modern non-parametric technique that offers the needed flexibility and frees the researcher from the limiting concept of a strict parametric shape. Although GAMs are increasingly used in ecological studies e.g. to study spatial distribution (Lehmann et al. 2002; Katsanevakis 2007), they have not been used to model absolute growth.

Mortality of *P. nobilis* is not studied as frequently as absolute growth. No studies on the survival of the planktonic stages of *P. nobilis* have been conducted and the mortality of larvae is virtually unknown in Pinnidae. Small benthic juveniles are very fragile and although there are indications of decreasing mortality with age, as larger individuals are less vulnerable to many of their predators (Butler et al. 1993), the factors that may affect *P. nobilis* mortality rates during ontogeny need further investigation. García-March et al. (2007a; b) have reported total annual mortality of 23.7% and 44.4% at two depth zones of 13 and 6 m depth respectively in Moraira Bay (Spain) and reported declining mortality rates with size in the deep zone but increased mortality of larger individuals in the shallow zone, attributed to hydrodynamic stress due to increased wave action.

The aim of this study was to investigate the temporal patterns and the effect of shell size and depth on growth and mortality rates of *P. nobilis* in a known population in Lake Vouliagmeni (Korinthiakos Gulf, Greece) (Katsanevakis 2006a; 2007), using flexible generalized additive models. Fishing mortality was investigated separately from natural mortality, to assess the effect of poaching on the lake's population.

Materials and Methods

Study area

The *P. nobilis* population of Lake Vouliagmeni (Korinthiakos Gulf, Greece) was studied to estimate growth and mortality rates. Lake Vouliagmeni is a semi-closed embayment, located on the 'Perachora' Peninsula and is connected to the Korinthiakos Gulf through a narrow (18.7 m) and shallow (1.1 m maximum depth) channel that was dredged approximately a century ago (Fig. 2). Lake Vouliagmeni has a maximum length (E-W) of 1881 m, width (N-S) of 931 m, depth of 49 m, and a total surface area of 150.4 ha (Katsanevakis 2006a). *P. nobilis* in Lake Vouliagmeni is mostly restricted at depths <16 m (Katsanevakis 2006a; 2007) and the total abundance of the species in the lake in 2006 was estimated to be 6770 individuals, with a 95% confidence interval of 5460 – 8393 individuals (Katsanevakis 2007).

Fieldwork

In May 2005, 150 *P. nobilis* individuals in Lake Vouliagmeni were tagged by SCUBA diving. The tagged individuals were located on the northeastern part of the lake, where a hotspot of high density had been observed (Katsanevakis 2007). Tagging was conducted in two bathymetric zones, a shallow one at depths between 2.5 and 6.5 m, where 100 individuals were tagged, and a deeper one at depths between 9 and 12 m, where another 50 individuals were tagged. The exact depth of each individual was measured using the electronic depth meter of a diving computer (Suunto, Vyper). The year 2004 had bad recruitment for *P. nobilis* in the lake; only two individuals of age class 0+ were found, among the 150 initially tagged individuals. During 2005, recruitment of *P. nobilis* in the lake was successful, and to gain extra data for small sizes, 10 more individuals of 0+ age class were located during spring – early summer of 2006 and tagged (all of them in the shallow bathymetric zone).

After their initial tagging and on a monthly basis, the width w (Fig. 3) of all tagged individuals was measured *in situ* with an aluminium vernier caliper (60 cm upper limit, 0.5 cm accuracy) for individuals with $w > 15$ cm or with a plastic vernier caliper (15 cm upper limit, 0.05 cm accuracy) for individuals with $w \leq 15$ cm. Monthly recording of the width of tagged individuals lasted from May 2005 to September 2006. The width of *P. nobilis* was measured instead of the length L (which is usually measured for absolute growth) because length measurements *in situ* would require uprooting the individuals to be measured and then replanting them in the same position for future measurements. Such a procedure would cause substantial disturbance that could affect subsequent growth rates and it would be very time-consuming, which would be prohibiting due to time-limitations of SCUBA diving.

Two kinds of mortality were recorded, natural and (illegal) fishing mortality. When an individual was found dead (an empty open shell) in its initial position, this was recorded as a natural mortality event. When an individual had been removed from its initial position, it was recorded as a fishing mortality event.

Estimation of growth and mortality rates

With a time span Δt of one month, instantaneous growth rates $gr = \frac{\mathrm{d}w}{\mathrm{d}t}$ were approximated as $\hat{gr} = \frac{\Delta w}{\Delta t} \approx \frac{\mathrm{d}w}{\mathrm{d}t}$, where $\Delta w = w_{t+\Delta t/2} - w_{t-\Delta t/2}$ is the growth in width during Δt. The estimated growth rate is considered to be valid at time t, which is the

midpoint of Δt. A Δt of one month was considered long enough to have detectable size changes and sufficiently small to achieve a satisfactory approximation of the instantaneous growth rate.

To model finite fishing mortality rate, a binary variable m_f was created, which for each individual had a value of 0 at time t, if during the interval [t - Δt/2, t + Δt/2] the individual had not been fished (i.e. was either alive or had died from natural causes), or a value of 1, if it had been fished. The expectation $E[\hat{m}_f]$ was the probability of death during Δt, or equivalently (because Δt was one month) the finite monthly fishing mortality rate (in mo^{-1}). Similarly, a binary variable m_n was defined that took a value of 0 at time t, if during the interval [t - Δt/2, t + Δt/2] the individual had not died by natural causes (i.e. was either alive or had been fished), or a value of 1, if it had died by natural causes. The expectation $E[\hat{m}_n]$ was the finite monthly natural mortality rate (in mo^{-1}).

Modelling growth and mortality

An information theory approach was followed in data analysis. According to the information theory approach, data analysis is taken to mean the integrated process of *a priori* specification of a set of candidate models (based on the science of the problem), model selection based on the principle of parsimony, and the estimation of parameters and their precision. The principle of parsimony implies the selection of a model with the smallest possible number of parameters for adequate representation of the data, a bias versus variance tradeoff.

All the mentioned growth differential equations (VBGM, Gompertz, logistic) were of the form $\frac{\mathrm{d}w}{\mathrm{d}t} = k \cdot g(w)$, where the relative growth rate parameter k was considered constant. In the general case k is a function of time and may also depend on other covariates x_i. Thus the differential equation becomes $\frac{\mathrm{d}w}{\mathrm{d}t} = k(t, x_1, x_2, ...) \cdot g(w)$. Assuming that $k(t, x_1, x_2, ...) = m_0(t) \cdot m_1(x_1) \cdot m_2(x_2) \cdots$, i.e. the relative growth parameter may be written as a product of one-variable functions of t, x_1, x_2,..., the instantaneous growth rate gr is given by the equation $gr = \frac{\mathrm{d}w}{\mathrm{d}t} = m_o(t) \cdot \prod_i m_i(x_i) \cdot g(w)$. By taking natural logarithms on both sizes of this equation to transform the product into a sum, it becomes $\log(gr) = \log(m_o(t)) + \sum_i \log(m_i(x_i)) + \log(g(w))$, which is written in condensed form as

$$\log(gr) = \sum_m r_m(z_m), \qquad \text{(Eq. 1)}$$

where z_m are the covariates (including w and t) and r_m are functions of these covariates. Equation 1 was modelled using generalized additive models (GAMs; Hastie and Tibshirani 1990), according to the general formulation:

$$f\left(E[\hat{gr}_i]\right) = LP_i = c + \sum_m s_m(z_{mi}), \qquad \text{(Eq. 2)}$$

where f is the link function, LP is the linear predictor, c is the intercept, $s_m(\cdot)$ is the one-dimensional smooth function of covariate z_m, and z_{mi} is the value of covariate m

for the *i*-th observation (Wood 2006). The log link was used, as suggested by Eq. 1, so that the predictor variables (through their smooth functions) would have a multiplicative effect on the response variable, and a Gaussian error distribution, which allows for negative values. Negative values of *gr* in the dataset, might be due either to abrasion of the shell (the outline of the shell is fragile and small pieces may peel off) or measurement error.

Three covariates were used as potential predictors of *gr*: the size (width) w_i of each *P. nobilis* individual, the time t_i of the year (in days) with 1 corresponding to 1/1/2005 (*t* ranged between 163 and 605), and the depth d_i, at which each individual was anchored. Depth was included as a covariate because depth-related variation in growth rates has been previously reported for another *P. nobilis* population (García-March et al. 2007a). Eight models q_j (j = 0 to 7), including all possible combinations of the three covariates were fitted (q_0 was the null model and q_1 was the full model).

The mortality rate (either m_f or m_n) was modelled using GAM, according to the general formulation:

$$f\left(E[\hat{m}_i]\right) = LP_i = c + \sum_m s_m(z_{mi}) \qquad \text{(Eq. 3)}$$

where the same covariates z_m were used as before (*w*, *t*, and *d*). A binomial error distribution was assumed and a logit link (canonical link for the binomial family) was used, where $f(E[\hat{m}_i]) = \log\left(E[\hat{m}_i] \big/ 1 - E[\hat{m}_i]\right)$, i.e. the natural logarithm of the odds of mortality. Eight models u_j and v_j (j = 0 to 7) for fishing and natural mortality respectively were fitted, including all possible combinations of the three covariates (j = 0 corresponds to the null model and j = 1 to the full model).

The smooth functions $s_m(\cdot)$ in Eqs 2 and 3 were represented using penalized regression splines (thin plate regression splines with basis dimension B = 15), estimated by penalized iterative least squares (Wood 2006). The optimum degree of smoothing was defined by Generalized Cross Validation (GCV) in the case of Eq. 2 and by minimizing the Un-Biased Risk Estimator (UBRE; Craven and Wahba 1979) in the case of Eq. 3, increasing the amount that each model effective degree of freedom counts in the GCV or UBRE score by a factor of $\gamma = 1.4$. UBRE is used when the scale parameter is known (binomial case of Eq. 3) and GCV is used when it is unknown (Gaussian error distribution of Eq. 2) (Wood 2006). GCV and UBRE are known to have some tendency for occasional overfitting, and it has been suggested that using $\gamma \approx 1.4$ can largely correct this without compromising the model fit (Kim and Gu 2004; Wood 2006). For generalized additive modelling, the package *mgcv* (Wood 2000; 2006) was used in R v.2.4.0 (R Development Core Team 2006).

Akaike Information Criterion (AIC) (Akaike 1973; Burnham and Anderson 2002) was used for model selection among the set of candidate models. The model with the smallest AIC value (AIC_{min}) was selected as the 'best' among the models tested. The AIC differences, $\Delta_i = AIC_i - AIC_{min}$, were computed over all candidate models. According to Burnham and Anderson (2002), models with $\Delta_i > 10$ have essentially no support and might be omitted from further consideration, models with $\Delta_i < 2$ have substantial support, while there is considerably less support for models with $4 < \Delta_i < 7$. To quantify the plausibility of each model, given the data and the set of five models, the 'Akaike weight' w_i of each model was calculated, which is considered as the weight of evidence in favor of model *i* being the actual best model of the available set of models (e.g. Akaike 1983; Buckland et al. 1997; Burnham and Anderson 2002).

Results

Growth rates

The best among the set of candidate models for growth rates was q_2 (Table 1). The full model (q_1) also had substantial support by the data ($\Delta_1 < 2$, $w_1 = 41.3\%$) but it explained the same amount of deviance as q_2 (with q_2 being nested to q_1), had a lower GCV score, and *s(d)* was found non-significant in q_1 (F-test, p = 0.134). For these reasons, q_2 was the single model selected for inference. The expression of q_2 was $\log\left(\hat{E[gr]} \right) = c + s_1(t) + s_2(w)$, where c = -5.48 ± 0.18 (± SE) and the smooth functions s_i are given graphically in Fig. 4. Growth rates had a peak at a width of ~4.5 cm, then sharply declined and remained approximately constant at sizes between 9 and 15 cm, and further declined at larger sizes becoming almost zero at w > 20 cm. There was an extended period of very low growth rates from early November 2005 to mid-March 2006 (t between 305 and 445), i.e. during the cold season. Another period of low growth rates was during August, both in 2005 and 2006 (t around 220 and 600 respectively), while peaks in growth rates were observed during late spring – early summer, both in 2005 and 2006 (t around 160 and 500 respectively) and also in September 2005 (t around 270) (Fig. 4).

Mortality

From May 2005 till the end of the survey on September 2006, 62 individuals were poached and 7 died by natural causes, among the 160 tagged individuals. Among the 62 fished individuals, 61 were in the shallow zone.

The best among the set of candidate models for fishing mortality (with no other model having support by the data) was u_1, i.e. the full model (Table 2). The expression of u_1 was $\mathrm{logit}\left(E[\hat{m}_f]\right) = c + s_1(t) + s_2(w) + s_3(d)$, where c = -6.24 ± 0.83 (± SE) and the smooth functions s_i are given graphically in Fig. 5. The shallower and the larger the size of *P. nobilis*, the higher the increase was in fishing mortality. Illegal fishing of *P. nobilis* occurred almost exclusively during the hot season (summer and early autumn), as depicted by the two peaks of *s(t)* during the hot seasons of 2005 and 2006 (Fig. 5).

The best among the set of candidate models for natural mortality was v_2 (Table 2). The full model (v_1) was ranked second and also had substantial support by the data ($\Delta_1 < 2$, $w_1 = 39.3\%$) but it explained only a slightly greater amount of deviance as v_2 (with v_2 being nested to v_1), had a lower UBRE score, and *s(d)* was found non-significant in v_1 (F-test, p = 0.247). For these reasons, v_2 was the single model selected for inference. The expression of v_2 was $\mathrm{logit}\left(E[\hat{m}_n]\right) = c + s_1(t) + s_2(w)$, where c = -7.66 ± 0.91 (± SE) and the smooth functions s_i are given graphically in Fig. 6. Natural mortality was much higher for younger and smaller individuals and diminished with size, and the period of highest natural mortality was summer and early autumn of 2006 (Fig. 6). Because of the low number of deaths by natural causes, definite conclusions regarding the importance of the candidate predictors of m_n may not be made; model v_2 is the best that can be inferred from the available dataset.

Specific values of mortality may be evaluated graphically from Figs 5 and 6. For example, to estimate finite fishing mortality rate during the summer peak in 2005, for individuals with a size of w = 20 cm at a depth of d = 4 m, we have $\text{logit}\left(E[\hat{m}_f]\right) = -6.24 + s_1(t = 245) + s_2(w = 20) + s_3(d = 4)$ or equivalently $\frac{E[\hat{m}_f]}{1 - E[\hat{m}_f]} = \exp(-6.24) \cdot \exp\left(s_1(t = 245)\right) \cdot \exp\left(s_2(w = 20)\right) \cdot \exp\left(s_3(d = 4)\right) = 0.00195A$, where A is the product of the corresponding values of the smooths on the 'odds-to-mortality' scale (right panel of Fig. 5). In this example, $\exp\left(s_1(t = 245)\right) = 26.93$, $\exp\left(s_2(w = 20)\right) = 10.94$, $\exp\left(s_3(d = 4)\right) = 8.37$, and thus A = 2465.9 and $\frac{E[\hat{m}_f]}{1 - E[\hat{m}_f]} = 4.809 \Rightarrow E[\hat{m}_f] = 0.828$. Finite mortality rates and their corresponding standard errors may be predicted using the *predict.gam* function in the package *mgcv* (Wood 2000; 2006) in R v.2.4.0 (R Development Core Team 2006). Using *predict.gam* it was found for this example that $E[\hat{m}_f] = 0.828 \pm 0.109$ (estimation ± SE). This finite monthly fishing mortality rate may be converted to a finite daily fishing mortality rate using the formula $(1 - m_1) = (1 - m_{30})^{1/30}$, where m_1 and m_{30} are finite mortality rates over a time interval of 1 or 30 days (i.e. one month) respectively (Krebs 1999). With the use of this formula, the estimated finite daily mortality rate was 0.0570, meaning that during the first days of September 2005, 5.7% of individuals with a width of 20 cm were poached each day from the 4-m depth zone, which is a very high mortality rate. Instantaneous mortality rates (μ) may also be calculated as $\mu = \log(1 - m)$ (Krebs 1999); for the above example, μ = -0.0587 day^{-1}.

Using *predict.gam*, finite daily total mortality rates $E[\hat{m}]$ were estimated for each day during the two-month period of August – September 2005, where a peak of fishing mortality was observed (Fig. 5). Finite daily survival rates were calculated as $1 - E[\hat{m}]$, and the product of all finite daily survival rates gave a total survival for that two-month period (Fig. 7). In just these two months, the majority of large individuals in shallow waters were poached (Fig. 7), contrary to deeper waters (≥ 10 m) where their survival was almost 100%.

Discussion

Food availability and temperature have been considered the main factors affecting growth and production in bivalves (Widdows et al. 1979; Rodhouse et al. 1984; McDonald and Thompson 1985; Page and Hubbard 1987; Thompson and Nichols 1988; Grant 1996; Urrutia et al. 1999; Shöne et al. 2003). In temperate regions, shell growth is favoured from late spring to early summer or even early autumn as a consequence of optimal nutritional conditions and temperatures, while it is very slow or absent during colder months. During spring and early summer in temperate regions, the availability of food (as a result of a major planktonic bloom) in combination with the increasing temperature pattern results in a main peak in shell growth. This has been found in many bivalve species, e.g. for *Ruditapes decussatus* (Urrutia et al. 1999), *Macoma balthica* (Bachelet 1980; Harvey and Vincent 1990), and *Placopecten magellanicus* (Grecian et al. 2000). Another (minor) planktonic bloom in autumn during the breakdown of the thermocline may also cause increased growth rates. However, in some coastal environments this classical pattern of annual

phytoplankton dynamics may not hold (e.g. Sinclair 1978; Legendre and Demers 1985). In Lake Vouliagmeni, *P. nobilis* had increased growth rates during late spring – early summer and also in autumn, while growth rates were minimal from late autumn to early spring. Hence, the seasonal growth pattern of the fan mussel was in accordance with the general observed pattern for bivalves in temperate regions. Most bivalves grow only within a certain temperature range and produce cessation marks if the temperature falls below or rises above the critical growth temperature limits (Shöne et al. 2003). Very high temperatures may slow down calcification significantly and exert a negative effect on shell growth due to increased metabolic costs or thermal stress (McDonald and Thompson 1985), which might be the cause of the observed decreased growth rates during August, when the water in the lake reached the highest temperature of the year, exceeding 29 ^{o}C.

The seasonal pattern of growth rates found in this study largely agrees with the results of Richardson et al. (1999) for two small fan mussels from Villaricos (Spain), for their two first years of life. They also found minimal growth rates during the cold period (November–March) and increased growth rates during late spring–summer. The only difference is that they did not find a cessation of growth at high temperatures, as was found in August for Lake Vouliagmeni. However, the estimated maximum temperature in Villaricos in late summer was ~25 ^{o}C, while in Lake Vouliagmeni surface temperature exceeded 29 ^{o}C. Maybe a temperature of 29 ^{o}C was high enough to cause cessation of growth contrary to the 25 ^{o}C of Villaricos. However, the effect of temperature should be viewed in combination with food availability and food quality. The spawning period of *P. nobilis* is during late summer – early autumn (Richardson et al. 1999) and spawning might also be a factor contributing to the halt in growth during August. Further investigation is needed to explain the observed August cessation of growth in Lake Vouliagmeni.

The pattern of growth rates in relation to individual size was more complicated than the patterns described by the classical models (VBGM, Gompertz, and logistic). There was a peak in growth rates at a relatively small size (w ~ 4.5 cm), which corresponds to individuals of age ~ 9 to 11 mo. This peak was much steeper than a Gompertz or a logistic model would predict and it was followed by approximately constant growth rates at sizes between 9 and 15 cm, which could not be predicted under anyone of the three classical models. It seems that if one of the classical models had been used (or even a model-average approach based on all three classical models), part of the information provided by the data would have been lost. The generalized additive modelling approach, being non-parametric and very flexible, is not restricted by specific forms and may reveal any type of pattern hidden in the dataset.

Many authors in many different areas have reported a depth-related size segregation of *P. nobilis* (Zavodnik 1967; Moreteau and Vicente 1982; Vicente 1990; Vicente and Moreteau 1991; Katsanevakis 2006a, 2007; García-March et al. 2007a, 2007b). The observed pattern was common: smaller individuals occurred more often in shallower waters, while larger individuals were concentrated deeper and were usually absent from the shallow waters. The hypothesis made by some researchers to explain this size segregation was that recruitment was favoured in shallower areas and then young individuals would move deeper towards ontogeny (Zavodnik 1967; Moreteau and Vicente 1982; Vicente and Moreteau 1991). García-March et al. (2007a) questioned this hypothesis and pointed out that there was no solid proof of the potential of young fan mussels to migrate deeper in any of the former studies. In their survey, they found no displacement or change of orientation of *P. nobilis* individuals

and reported that apart from the short period just after settlement, in which some movement may be possible, when an individual is large enough to be detected, it remains in the same position until its death. The same was observed in the present study, where none of the tagged individuals were found to change position. García-March et al. (2007a) underlined that displacement by using the foot, as is done by many Veneroida, is less probable in the Pinnidae because the foot is reduced and too small in relation to the shell size. Furthermore, they pointed out that crawling through the substratum, in a similar way to many other Pteriomorphia, either attaching new byssus filaments in the direction of movement and liberating older rear ones, or by shedding the entire byssus complex and producing a new one for re-implementation would also be difficult; *P. nobilis* would need 4–5 months to regenerate the dissected byssus, contrary to other mussels that have the ability to crawl, which are able to produce a new byssus complex in a few hours or days (Côté 1995; Uryu et al. 1996).

García-March et al. (2007a, 2007b) found that the size segregation in Moraira Bay existed because of higher mortality and lower asymptotic size in shallow compared to deep waters and attributed these differences in growth and mortality to hydrodynamic stress caused by the water flow produced by waves. In the present study, no depth-related differences were substantiated in growth or natural mortality rates. This difference between the two studies is largely because Lake Vouliagmeni is quite sheltered and contrary to Moraira Bay, the wave intensity is very low even in the very shallow waters, independent of the weather conditions. Thus fan mussels in the shallow areas of Lake Vouliagmeni do not suffer from high hydrodynamic stress as in Moraira Bay.

As depicted in Fig. 8, marked size segregation with depth was observed in Lake Vouliagmeni (Katsanevakis 2006; unpublished data) and was attributed exclusively to fishing mortality, according to the findings of the present study. The survival of large individuals in shallow waters was strikingly low due to fishing mortality, whilst at a depth of 12 m, large individuals did not suffer from poaching. In just a two month period (Fig. 7), mortality of individuals with $w > 18$ cm was > 80% at a depth of 4 m. Because of these high fishing mortalities in the shallow areas, *P. nobilis* individuals do not have the chance to grow large and most of them are poached at a size $w < 18$ cm, while in deeper areas the peak of the size-frequency distribution is larger than 18 cm (Fig. 8). Such size segregation of *P. nobilis*, due to fishing mortality has also been suggested by Vicente (1990).

Poaching of *P. nobilis* in Lake Vouliagmeni is conducted exclusively by free-diving. Given the low visibility in the lake (usually much less than 10 m), skin divers are generally restricted to shallow depths, which explains the declining fishing mortality with depth, which diminishes at depths >9 m (Fig 5). Furthermore, fishing mortality is greater during summer and early autumn, especially during August, as at that time the lake is crowded by summer visitors who spend their holidays by the lake and many of them collect fan mussels for food or for their shells, targeting mostly large individuals. On the contrary, during winter and spring, the lake is depopulated and the water is too cold for free-diving, which explains the temporal pattern of fishing mortality. The effect of fishing mortality on the density and spatial distribution of *P. nobilis* is huge, resulting in a bimodal bathymetric distribution of the species with one peak at depths between 13 and 15 m, consisting mainly of large individuals, and another smaller peak in the 4-m zone, consisting mainly of small individuals of ages <4 yr (Katsanevakis 2006a, 2007). If there was no fishing mortality in the shallow zone and because recruitment is more successful in the shallow zone of the

Lake, the spatial distribution and the density surface would probably be completely different with densities higher in the shallow zone, declining with depth.

Natural mortality was much lower than fishing mortality and was mainly size-defined, with young individuals suffering much higher mortality rates than adults. The smooth of size *s(w)* in model v_2 was linear and thus the equation relating natural mortality rates and size (for a constant time *t*) was of the form $\text{logit}(E[\hat{m}_n]) = a_0 + a_1 w$ or equivalently $E[\hat{m}_n] = \frac{\exp(a_0 + a_1 w)}{1 + \exp(a_0 + a_1 w)}$, where $a_0 > 0$ and $a_1 < 0$ are constants. A reduction of mortality with size seems to be the rule for most bivalves. Many other field studies on the life history of marine bivalves have also indicated that survivorship is size-dependent: lower at small sizes and higher as the bivalves grow larger (e.g. Brousseau 1978; Nakaoka 1996). In particular, bivalves sometimes abruptly reduce their natural mortality due to predation or physical stress after reaching a critical size, which is called the 'refuge size' (Levinton and Bambach 1969; Seed 1993; Nakaoka 1996; Nakaoka 1998). It seems that for *P. nobilis* such a 'refuge size' is a *w* of ~8 cm, i.e. high mortality affects mostly the individuals during their first year of age (which in Lake Vouliagmeni have a width <8 cm (Katsanevakis 2006a)).

In this study, the use of GAMs as a tool to analyze growth and mortality data was demonstrated. This approach is novel and beneficial as opposed to the usual parametric approaches. The use of GAMs allows the exploration of shapes of growth and mortality response curves in relation to predictor variables and allows the fitting of statistical models that better agree with ecological theory and are not restricted by convenient mathematical formulas. The ecological interpretability of the non-parametric response curves and the flexibility of GAMs to fit the data closely are advantageous characteristics that make them a valuable tool in marine ecological studies.

Acknowledgements

I would like to thank two anonymous reviewers for their suggestions and comments, which helped to improve the quality of the manuscript. This work complies with the current laws of Greece and EU.

References

Akaike H (1973) Information theory and an extension of the maximum likelihood principle. In: Petrov BN, Csàaki F (eds) Second international symposium on information theory. Akademiai Kiado, Budapest, pp 267–281

Akaike H (1983) Information measures and model selection. B Int Stat Inst 44:277-291

Bachelet G (1980) Growth and Recruitment of the Tellinid Bivalve *Macoma balthica* at the Southern Limit of Its Geographical Distribution, the Gironde Estuary (SW France). Mar Biol 59:105–117

Bertalanffy von L (1938) A quantitative theory of organic growth (Inquiries on growth laws II). Human Biol 10:181–213

Brousseau DJ (1978) Population dynamics of the soft-shell clam *Mya arenaria*. Mar Biol 50:63–71

Buckland ST, Burnham KP, Augustin NH (1997) Model selection: an integral part of inference. Biometrics 53:603–618.

Burnham KP, Anderson DR (2002) Model selection and multimodel inference: a practical information-theoretic approach, 2nd edn. Springer, Berlin

Butler AJ, Vincente N, Gaulejac B de (1993) Ecology of the pteroid bivalves *Pinna bicolor* Gmelin and *Pinna nobilis* L. Mar Life 3:37–45

Côté IM (1995) Effects of predatory crab effluent on byssus production in mussels. J Exp Mar Biol Ecol 188:233–241

Craven P, Wahba G (1979) Smoothing noisy data with spline functions, Numerische Mathematik 31:377-403

Galinou-Mitsoudi S, Vlahavas G, Papoutsi O (2006) Population study of the protected bivalve *Pinna nobilis* (Linaeus, 1758) in Thermaikos Gulf (North Aegean Sea). J Biol Res 5:47–53

García-March JR, García-Carrascosa AM, Peña Cantero AL, Wang YG (2007a) Population structure, mortality and growth of *Pinna nobilis* Linnaeus, 1758 (Mollusca: Bivalvia) at different depths in Moraira Bay (Alicante, Western Mediterranean). Mar Biol 150:861–871

García-March JR, Pérez-Rojas L, García-Carrascosa AM (2007b) Influence of hydrodynamic forces on population structure of *Pinna nobilis* L., 1758 (Mollusca: Bivalvia): The critical combination of drag force, water depth, shell size and orientation. J Exp Mar Biol Ecol 342:202–212

Gompertz B (1825) On the nature of the function expressive of the law of human mortality and on a new mode of determining the value of life contingencies. Phil Trans R Soc London 115:515–585

Grant J (1996) The relationship of bioenergetics and the environment to the field growth of cultured bivalves. J Exp Mar Biol Ecol 200:239–256

Grecian LA, Parsons J, Dabinett P, Couturier C (2000) Influence of season, initial size, depth, gear type and stocking density on the growth rates and recovery of sea scallop, *Placopecten magellancius*, on a farm-based nursery. Aquacult Int 8:183–206

Harvey M, Vincent B (1990) Density, size distribution, energy allocation and seasonal variations in shell and soft tissue growth at two tidal levels of a *Macoma balthica* (L.) population. J Exp Mar Biol Ecol 142:151–168

Hastie TJ, Tibshirani RJ (1990) Generalized Additive Models. Chapman and Hall, London

Katsanevakis S (2006a) Population ecology of the endangered fan mussel *Pinna nobilis* in a marine lake. Endang Species Res 1:51–59

Katsanevakis S (2006b) Modelling fish growth: model selection, multi-model inference and model selection uncertainty. Fish Res 81:229–235

Katsanevakis S (2007) Density surface modelling with line transect sampling as a tool for abundance estimation of marine benthic species: the *Pinna nobilis* example in a marine lake. Mar Biol, in press. DOI 10.1007/s00227-007-0659-3

Kim YJ, Gu C (2004) Smoothing spline gaussian regression: more scalable computation via eficient approximation. J Roy Stat Soc B 66:337–356

Krebs CJ (1999) Ecological methodology, 2nd edn. Addison Welsey Longman, New York

Legendre L, Demers S (1985) Auxiliary energy, ergoclines and aquatic biological production. Nat Can 112:5–14

Lehmann A, Overton J McC, Leathwick JR (2002) GRASP: generalized regression analysis and spatial prediction. Ecol Model 157:189–207

Levinton JS, Bambach RK (1969) Some ecological aspects of bivalve mortality patterns. Am J Sci 268:97–112

Lessa R, Duarte-Neto P (2004) Age and growth of yellowfin tuna (*Thunnus albacares*) in the western equatorial Atlantic, using dorsal fin spines. Fish Res 69:157–170

McDonald BA, Thompson RJ (1985) Influence of temperature and food availability on the ecological energetics of the giant scallop *Placopecten magellanicus*. I. Growth rates of shell and somatic tissue. Mar Ecol Prog Ser 25:279–294

Moreteau JC, Vicente N (1982) Evolution d'une population de *Pinna nobilis* L. (Mollusca, Bivalvia). Malacologia 22:341–345

Nakaoka M (1996) Size-dependent survivorship of the bivalve *Yoldia notabilis* (Yokoyama, 1920): The effect of crab predation. J Shellfish Res 15:355–362

Nakaoka M (1998) Optimal resource allocation of the marine bivalve Yoldia notabilis: The effects of size-limited reproductive capacity and size-dependent mortality. Evol Ecol 12:347–361

Page HM, Hubbard DM (1987) Temporal and spatial patterns of growth in mussels *Mytilus edulis* on an offshore platform: relationships to water temperature and food availability. J Exp Mar Biol Ecol 111:159–179

Ramos MA (1998) Impementing the habitats directive for mollusk species in Spain. J Concol Spec Publ 2:125–132

R Development Core Team (2006). R: A language and environment for statistical computing. R Foundation for Statistical Computing, Vienna, Austria. ISBN 3-900051-07-0, URL http://www.R-project.org

Richardson CA, Kennedy H, Duarte CM, Kennedy DP, Proud SV (1999) Age and growth of the fan mussel *Pinna nobilis* from south-east Spanish Mediterranean seagrass (*Posidonia oceanica*) meadows. Mar Biol 133:205–212

Richardson CA, Peharda M, Kennedy H, Kennedy P, Onofri V (2004) Age, growth rate and season of recruitment of *Pinna nobilis* (L) in the Croatian Adriatic determined from Mg:Ca and Sr:Ca shell profiles. J Exp Mar Biol Ecol 299:1–16

Ricker WE (1975) Computation and interpretation of biological statistics of fish populations. Bull Fish Res Bd Can 191:1–382

Rodhouse PG, Roden CM, Bumell GM, Hensey MP, McMahon T, Ottway B, Ryan TH (1984) Food resource, gametogenesis and growth of *Mytilus edulis* on the shore and in suspended culture in Killary Harbour, Ireland. J Mar Biol Assoc UK 64:513-529

Seed R (1993) Invertebrate predators and their role in structuring coastal and estuarine populations of filter feeding bivalves. In: Dame RF (ed) Bivalve Filter Feeders in Estuarine and Coastal Ecosystem Processes. Springer-Verlag, Berlin, pp. 149–195

Shöne B, Tanabe K, Dettman D, Sato S (2003) Environmental controls on shell growth rates and $\delta^{18}O$ of the shallow-marine bivalve mollusk *Phacosoma japonicum* in Japan. Mar Biol 142:473–485

Šiletić T, Peharda M (2003) Population study of the fan shell *Pinna nobilis* L. in Malo and Veliko Jezero of the Mljet National Park (Adriatic Sea). Sci Mar 67:91–98

Sinclair M (1978) Summer phytoplankton variability in the Lower St. Lawrence Estuary. J Fish Res Bd Can 35:1171–1185

Thompson JK, Nichols FH (1988) Food availability controls seasonal cycle of growth in *Macoma balthica* (L.) in San Francisco Bay, California. J Exp Mar Biol Ecol 116:43–61

Urrutia MB, Ibarrola I, Iglesias JIP, Navarro E (1999) Energetics of growth and reproduction in a high-tidal population of the clam *Ruditapes decussatus* from Urdaibai Estuary (Basque Country, N. Spain). J Sea Res 42:35–48

Uryu Y, Iwasaki K, Hinoue M (1996) Laboratory experiments on behaviour and movements of a freshwater mussel, *Limnoperna fortunei* (Dunker). J Mollus Stud 62:327–341

Vicente N (1990) Estudio ecológico y protección del molusco lamelibranquio *Pinna nobilis* L. 1758 en la costa mediterránea. Iberus 9:269–279

Vicente N, Moreteau JC (1991) Statut de *Pinna nobilis* L. en Mediterranee (mollusque eulamellibranche). In: Boudouresque CF, Avon M, Gravez V (eds) Les espèces marines à protéger en Méditerranée. GIS Posidonie publ., Marseille, pp. 159–168

Widdows J, Fieth P, Worrall CM (1979). Relationship between seston, available food and feeding activity in the common mussel *Mytilus edulis*. Mar Biol 50:195-207.

Wood SN (2000) Modelling and smoothing parameter estimation with multiple quadratic penalties. J R Stat Soc, Series B, 62:413–428

Wood SN (2006) Generalized Additive Models: An introduction with R. Chapman and Hall/CRC, Florida

Yamaguchi M (1975) Estimating growth parameters from growth rate data: problems with marine sedentary invertebrates. Oecologia 20:321–332

Zavodnik D (1967) Contribution to the ecology of *Pinna nobilis* L. (Moll., Bivalvia) in the Northern Adriatic. Thalassia Yugosl 3:93–102

Zavodnik D, Hrs-Brenko M, Legac M (1991) Synopsis on the fan shell *Pinna nobilis* L. in the eastern Adriatic Sea. In: Boudouresque CF, Avon M, Gravez V (eds) Les Espèces Marines à Protéger en Méditerranée. GIS Posidonie publ., Marseille, pp 169–178

Figure legends

Fig. 1: Size specific growth rates of Yellowfin tuna based on different growth models: Von Bertalanffy Growth Model (VBGM), Gompertz, and Logistic.

Fig. 2: Map of Lake Vouliagmeni. The area in which the *P. nobilis* individuals were tagged is indicated (Study Area) and also the bathymetric contours of the lake (at 5-m intervals).

Fig. 3: *Pinna nobilis*. The width w and length L are indicated.

Fig. 4: Estimated smooth terms for the q_2 model of *Pinna nobilis* instantaneous growth rates. In the left panel, the smooth terms are given in the linear predictor scale (i.e. in $\log gr$) and the corresponding 95% confidence intervals are given with dotted lines, while in the right panel the smooth terms are given in the response scale (i.e. smooth terms were exp-transformed). The number *edf* in $s(z_m, edf)$ is the estimated degrees of freedom of the smooth term. A one-dimensional scatterplot is given at the bottom of each graph, using a vertical bar as the plotting symbol, to illustrate the distribution of available data.

Fig. 5: Estimated smooth terms for the u_1 model of *Pinna nobilis* finite monthly fishing mortality rates. In the left panel, the smooth terms are given in the linear predictor scale (i.e. in $\log\left(E[\hat{m}_i] / 1 - E[\hat{m}_i]\right)$) and the corresponding 95% confidence intervals are given with dotted lines, while in the right panel the smooth terms are given in the 'odds of mortality' scale (i.e. in $E[\hat{m}_i] / 1 - E[\hat{m}_i]$). The number *edf* in $s(z_m, edf)$ is the estimated degrees of freedom of the smooth term. A one-dimensional scatterplot is given at the bottom of each graph, using a vertical bar as the plotting symbol, to illustrate the distribution of available data. A positive effect on mortality rates occurs when $s(\cdot) > 0$ in the linear predictor scale or > 1 in the 'odds of mortality' scale, while a negative effect occurs when $s(\cdot) < 0$ in the linear predictor scale or < 1 in the 'odds of mortality' scale.

Fig. 6: Estimated smooth terms for the v_2 model of *Pinna nobilis* finite monthly natural mortality rates. In the left panel, the smooth terms are given in the linear predictor scale (i.e. in $\log\left(E[\hat{m}_i] / 1 - E[\hat{m}_i]\right)$) and the corresponding 95% confidence intervals are given with dotted lines, while in the right panel the smooth terms are given in the 'odds of mortality' scale (i.e. in $E[\hat{m}_i] / 1 - E[\hat{m}_i]$). The number *edf* in $s(z_m, edf)$ is the estimated degrees of freedom of the smooth term. A one-dimensional scatterplot is given at the bottom of each graph, using a vertical bar as the plotting symbol, to illustrate the distribution of available data. A positive effect on mortality rates occurs when $s(\cdot) > 0$ in the linear predictor scale or > 1 in the 'odds of mortality' scale, while a negative effect occurs when $s(\cdot) < 0$ in the linear predictor scale or < 1 in the 'odds of mortality' scale.

Fig. 7: Size specific survival of *P. nobilis* during August – September 2005 at various depths, conditional on models u_1 and v_2 for fishing and natural mortality rates respectively.

Fig. 8: Size-frequency distribution of width *w* of *P. nobilis* shells at two depth zones (< 7 m and > 9 m) during July of three consecutive years (2004–2006). The data for 2004 are from Katsanevakis (2006a), while data for 2005 and 2006 are unpublished.

Table 1: Evaluation of candidate models (q_i) for growth rates (gr) based on Akaike Information Criterion (AIC). Models were sorted from best to worst. Estimated degrees of freedom (edf), generalized cross validation (GCV) scores, percentage of deviance explained, AIC differences (Δi), and Akaike weights (w_i) are also given.

Model	Linear Predictor	edf	Deviance Explained (%)	GCV	AIC	Δ_i	w_i (%)
q_2	*c + s(t) + s(w)*	23.2	26.7	0.0001353	-9109.5	0.0	58.7
q_1	*c + s(t) + s(w) + s(d)*	23.9	26.7	0.0001354	-9108.8	0.7	41.3
q_3	*c + s(t) + s(d)*	16.3	18.6	0.0001482	-8966.9	142.6	0.0
q_6	*c + s(w)*	12.8	14.4	0.0001543	-8902.0	207.6	0.0
q_4	*c + s(w) + s(d)*	9.2	13.7	0.0001546	-8894.1	215.4	0.0
q_5	*c + s(t)*	13.8	12.5	0.0001586	-8863.5	246.0	0.0
q_7	*c + s(d)*	3.0	5.1	0.0001685	-8763.8	345.7	0.0
q_0	*c*	2.0	0.0	0.0001773	-8687.3	422.2	0.0

Table 2: Evaluation of candidate models u_i and v_i for fishing and natural mortality respectively, based on Akaike Information Criterion (AIC). Models were sorted from best to worst. Estimated degrees of freedom (edf), un-biased risk estimator (UBRE) scores, percentage of deviance explained, AIC differences (Δi), and Akaike weights (w_i) are also given.

Model	Linear Predictor	edf	Deviance Explained (%)	UBRE	AIC	Δ_i	w_i (%)
Fishing mortality							
u_1	*c + s(t) + s(w) + s(d)*	10.3	35.3	-0.7704	360.4	0.0	100.0
u_3	*c + s(t) + s(d)*	9.3	30.6	-0.7567	383.2	22.8	0.0
u_2	*c + s(t) + s(w)*	12.4	27.8	-0.7423	403.9	43.5	0.0
u_5	*c + s(t)*	8.4	20.4	-0.7252	434.7	74.3	0.0
u_4	*c + s(w) + s(d)*	3.6	16.9	-0.7221	443.5	83.0	0.0
u_7	*c + s(d)*	2.0	9.0	-0.6990	481.9	121.5	0.0
u_6	*c + s(w)*	6.5	9.6	-0.6930	487.8	127.4	0.0
u_0	*c*	1.0	0.0	0.0011	527.1	166.7	0.0
Natural mortality							
v_2	*c + s(t) + s(w)*	4.2	41.4	-0.9599	61.1	0.0	60.2
v_1	*c + s(t) + s(w) + s(d)*	5.2	42.7	-0.9588	62.0	0.9	39.3
v_6	*c + s(w)*	2.0	24.8	-0.9543	71.7	10.6	0.3
v_4	*c + s(w) + s(d)*	3.0	25.9	-0.9532	72.7	11.6	0.2
v_5	*c + s(t)*	3.1	17.0	-0.9480	81.0	19.9	0.0
v_3	*c + s(t) + s(d)*	3.2	11.1	-0.9468	86.5	25.4	0.0
v_0	*c*	1.0	0.0	-0.0012	92.1	30.9	0.0
v_7	*c + s(d)*	2.0	1.7	-0.9414	92.6	31.4	0.0

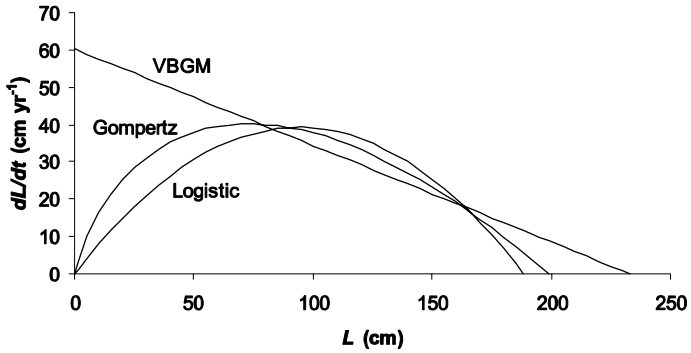
70
60
50
40
30
20
10
0
dL/dt (cm yr-1)
VBGM
Gompertz
Logistic
0
50
100
150
200
250
L (cm)

Fig. 1

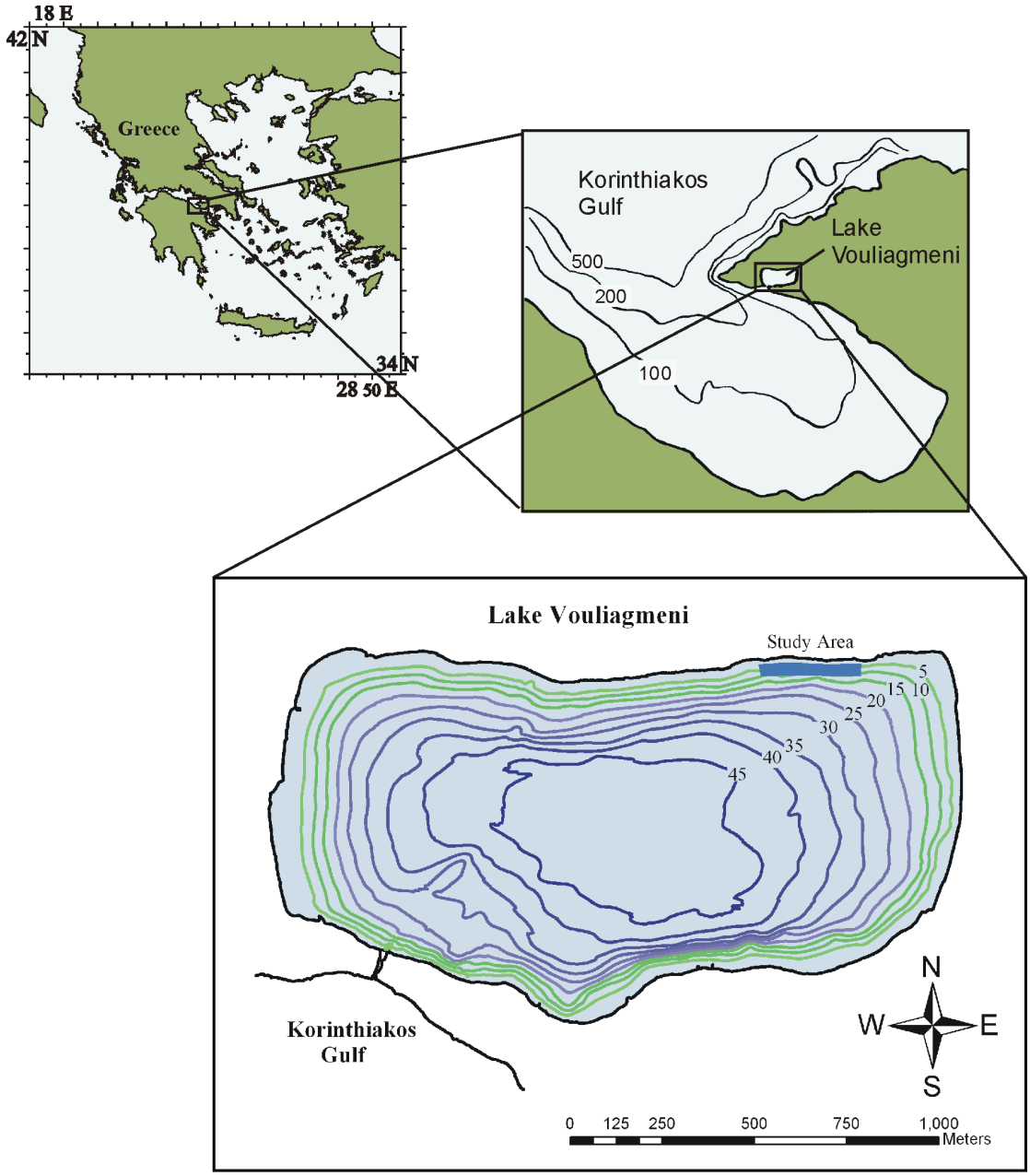
18 E
42 N
Greece
34 N
28 50 E
Korinthiakos
Gulf
Lake
Vouliagmeni
500
200
100
Lake Vouliagmeni
Study Area
5
10
15
20
25
30
35
40
45
Korinthiakos
Gulf
N
W
E
S
0 125 250 500 750 1,000
Meters

Fig. 2

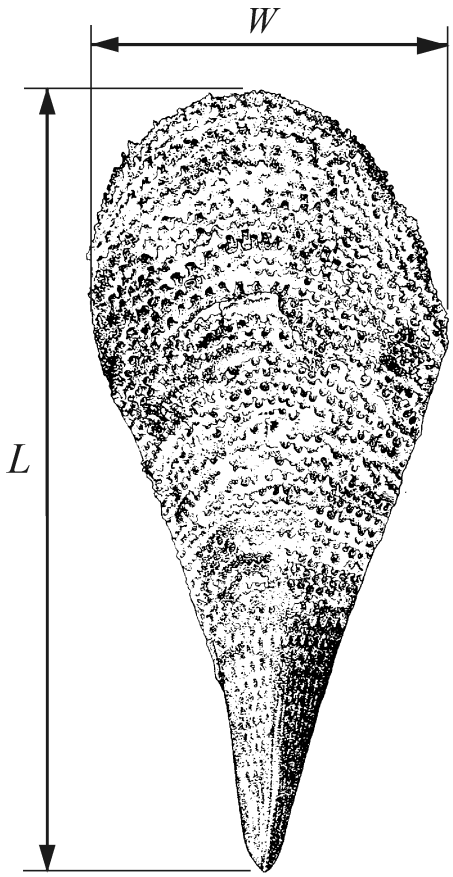

Fig. 3

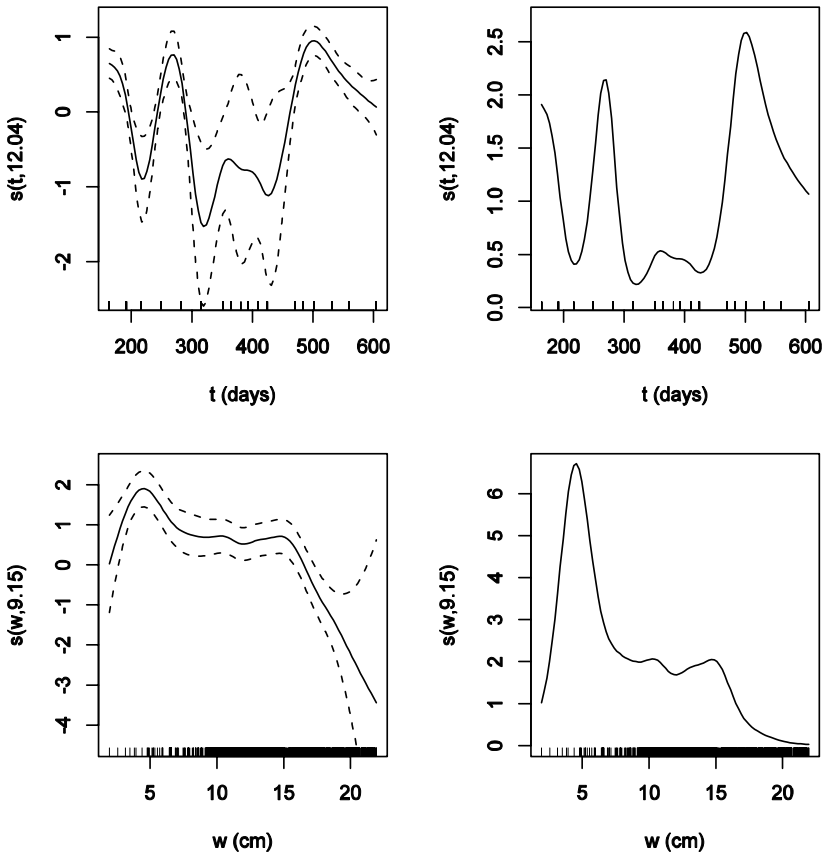

Fig. 4

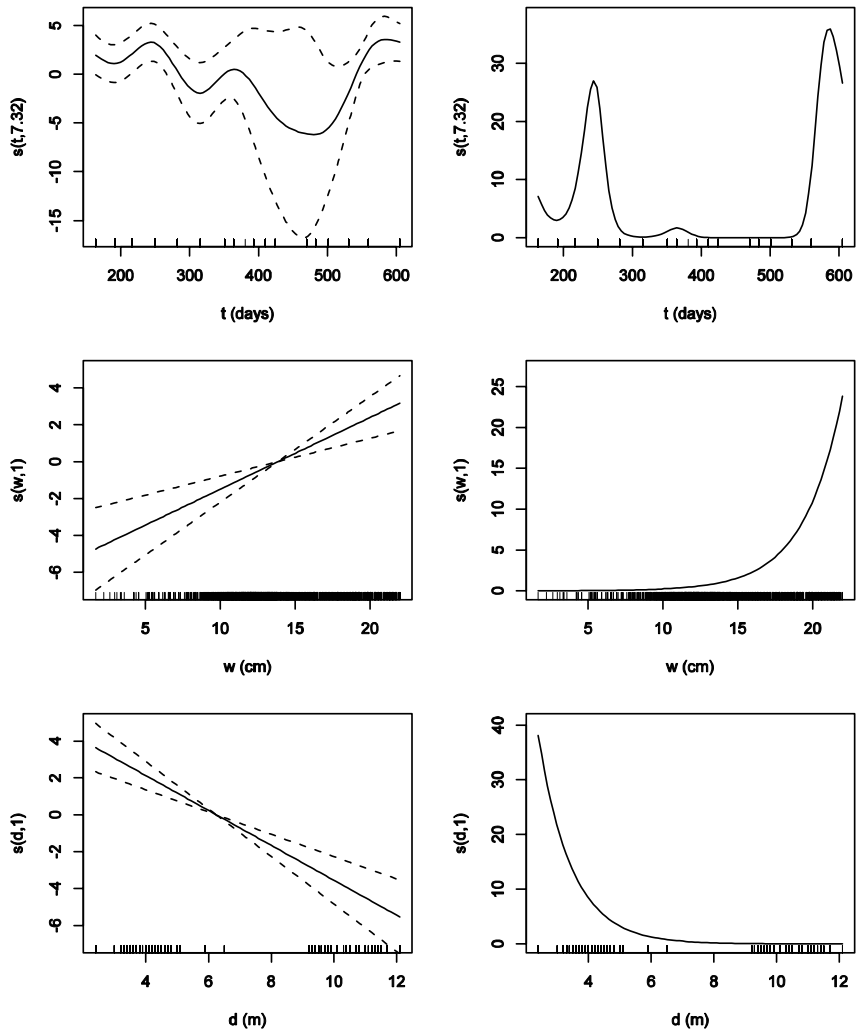

Fig. 5

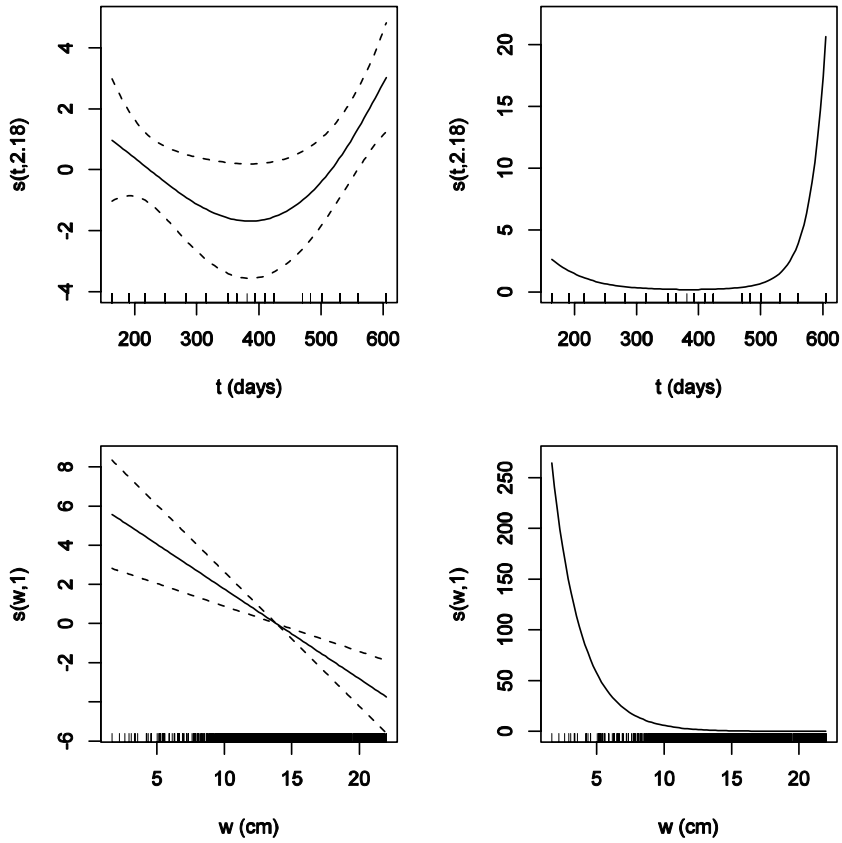
s(t,2.18)
t (days)
s(t,2.18)
t (days)
s(w,1)
w (cm)
s(w,1)
w (cm)

Fig. 6

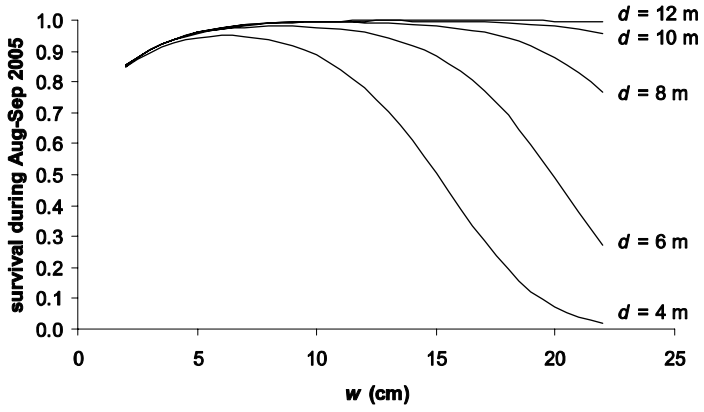
survival during Aug-Sep 2005
w (cm)
d = 12 m
d = 10 m
d = 8 m
d = 6 m
d = 4 m

Fig. 7

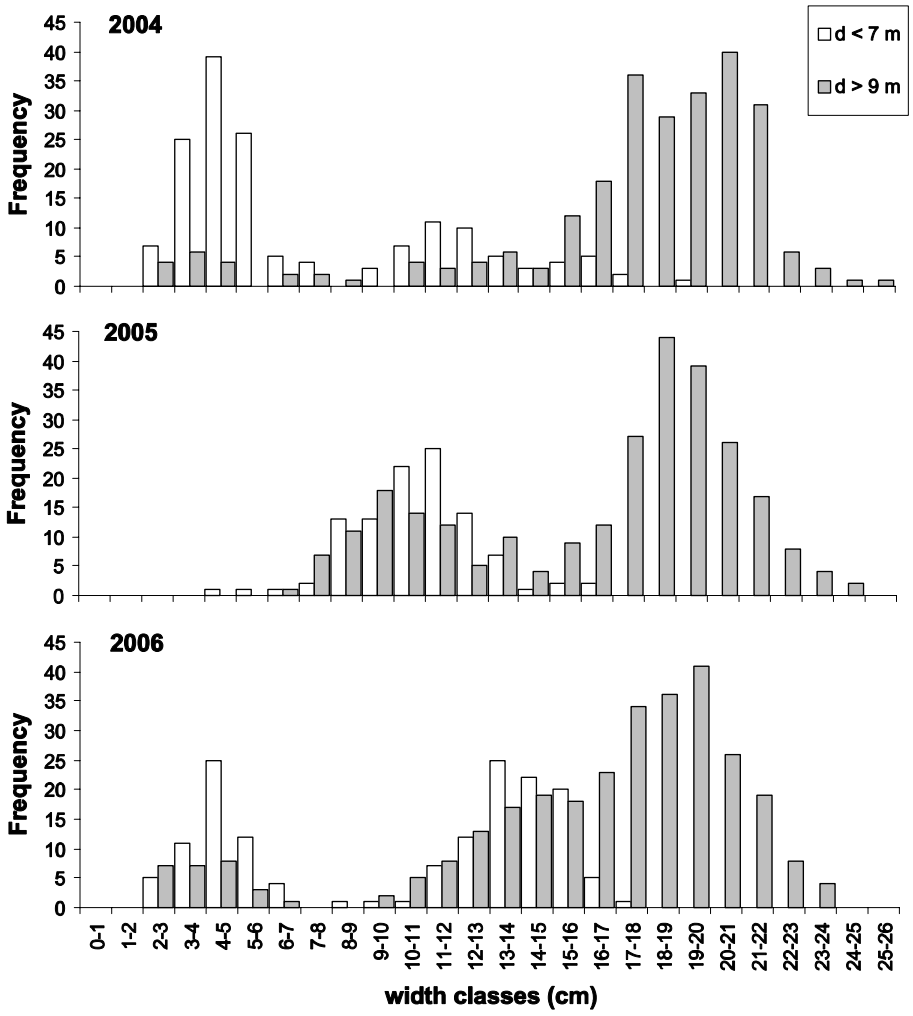
2004
2005
2006
Frequency
□d < 7 m
▩d > 9 m
0-1
1-2
2-3
3-4
4-5
5-6
6-7
7-8
8-9
9-10
10-11
11-12
12-13
13-14
14-15
15-16
16-17
17-18
18-19
19-20
20-21
21-22
22-23
23-24
24-25
25-26
width classes (cm)

Fig. 8